



Oxidative and nitrosative stress in the neurotoxicity of polybrominated diphenyl ether-153: possible mechanism and potential targeted intervention



Hongmei Zhang^{a,1}, Xiaorong Yang^{b,1}, Xin Li^c, Yan Cheng^d, Huajun Zhang^a, Lijun Chang^a, Min Sun^a, Zhihong Zhang^a, Zemin Wang^e, Qiao Niu^{f,*}, Tong Wang^{g,**}

^a Department of Environmental Health, Shanxi Medical University, Taiyuan, 030001, Shanxi, China

^b National Key Disciplines, Key Laboratory for Cellular Physiology of Ministry of Education, Department of Neurobiology, Shanxi Medical University, Taiyuan, 030001, Shanxi, China

^c Center of Disease Control and Prevention, Taiyuan Iron and Steel Company, Taiyuan, 030003, Shanxi, China

^d Department of Nuclear Medicine, First Affiliated Hospital of Shanxi Medical University, Taiyuan, 030001, Shanxi, China

^e Department of Environmental Health, Indiana University School of Public Health, Bloomington, IN, 47408, USA

^f Department of Occupational Health, Shanxi Medical University, Taiyuan, 030001, Shanxi, China

^g Department of Health Statistics, Shanxi Medical University, Taiyuan, 030001, Shanxi, China

H I G H L I G H T S

- BDE-153 can induce neurotoxicity in rats, however, the underlying mechanism and intervention are not clear.
- Brain is highly sensitive to oxidative or nitrosative stress.
- Oxidative and nitrosative stresses are the main mechanism of the neurotoxicity induced by BDE-153.
- And the antioxidation is a potential targeted intervention.

A R T I C L E I N F O

Article history:

Received 12 June 2019

Received in revised form

30 July 2019

Accepted 15 August 2019

Available online 16 August 2019

Handling Editor: A. Gies

Keywords:

Polybrominated diphenyl ether-153

Oxidative stress

Nitrosative stress

Neurotrophin

Cholinergic enzyme

Neurotoxicity

A B S T R A C T

Polybrominated diphenyl ethers (PBDEs) have been known to exhibit neurotoxicity in rats; however, the underlying mechanism remains unknown and there is no available intervention. In this study, we aimed to investigate the role of oxidative and nitrosative stress in the neurotoxicity in the cerebral cortex and primary neurons in rats following the BDE-153 treatment. Compared to the untreated group, BDE-153 treatment significantly induced the neurotoxic effects in rats, as manifested by the increased lactate dehydrogenase (LDH) activities and cell apoptosis rates, and the decreased neurotrophic factor contents and cholinergic enzyme activities in rats' cerebral cortices and primary neurons. When compared to the untreated group, the oxidative and nitrosative stress had occurred in the cerebral cortex or primary neurons in rats following the BDE-153 treatment, as manifested by the increments in levels of reactive oxygen species (ROS), malondialdehyde (MDA), nitric oxide (NO), and neuronal nitric oxide synthase (nNOS) mRNA and protein expressions, along with the decline in levels of superoxide dismutase (SOD) activity, glutathione (GSH) content, and peroxiredoxin I (Prx I) and Prx II mRNA and protein expressions. In addition, the ROS scavenger N-acetyl-L-cysteine (NAC) or NO scavenger NG-Nitro-L-arginine (L-NNA) significantly rescued the LDH leakage and cell survival, reversed the neurotrophin contents and cholinergic enzymes, mainly via regaining balance between oxidation/nitrosation and antioxidation. Overall, our findings suggested that oxidative and nitrosative stresses are involved in the neurotoxicity induced by BDE-153, and that the antioxidation is a potential targeted intervention.

© 2019 Published by Elsevier Ltd.

* Corresponding author. Department of Occupational Health, Shanxi Medical University, Xinjian South Ave 56, Taiyuan, 030001, China.

** Corresponding author. Department of Health Statistics, Shanxi Medical University, Xinjian South Ave 56, Taiyuan, 030001, China.

E-mail addresses: niuqiao55@sxmu.edu.cn (Q. Niu), tongwang@sxmu.edu.cn (T. Wang).

¹ Hongmei Zhang and Xiaorong Yang are the first co-authors.

1. Introduction

Polybrominated diphenyl ethers (PBDEs) were widely used in the manufacturing process of electronics, cables, furniture, carpets and textiles all over the world. Despite the PBDE usage in products had started out since 2004 (Penta- and Octa-PBDE) and 2013 (Deca-PBDE), people are still widely exposed to PBDEs via dust ingestion and dietary digestion (Hammel et al., 2017; Ni et al., 2013; Xu et al., 2018). Toddlers are exposed to higher dose of PBDEs than adults, and infants are exposed to a lot more PBDEs via breast-feeding (Johnson-Restrepo and Kannan, 2009; Jeong et al., 2014), especially those in North America where the highest PBDEs concentrations have been found (Zhang et al., 2017a). PBDEs are more readily transferred to rat pups via postnatal breastfeeding than placenta *in utero* (Shin et al., 2017), and the predominant congeners are BDE-47, BDE-153 and BDE-209 in humans (Tang and Zhai, 2017). Prenatal or postnatal PBDE concentrations are significantly associated with the decreased neurodevelopment scores in children across several birth cohorts from the US, Europe and Asia (Chen et al., 2014; Eskenazi et al., 2013; Herbstman et al., 2010; Roze et al., 2009; Chao et al., 2011). In rats and mice, perinatal administration of BDE-153 or other PBDE congener causes long-lasting learning and memory deficits, disrupts the habituation, and impairs the spontaneous behavior (Viberg et al., 2003, 2006; Zhang et al., 2013). Nevertheless, the underlying mechanism of neurotoxicity induced by BDE-153 and the potential targeted intervention are still need to be well understood.

Oxidative stress or nitrosative stress indicates the imbalance between production and quenching of reactive oxygen species (ROS) or reactive nitrogen species (RNS) within cells, and is usually indicated as an overproduction of ROS or RNS. ROS consist of $O_2^{\cdot-}$, H_2O_2 , HO_2 and $-OH$, are widely involved in the cell proliferation and differentiation, cell death, signal transduction, and oxidative damage. RNS are a series of nitric oxide (NO) derivatives produced from the reaction of NO with superoxide ($O_2^{\cdot-}$). Nitrosative stress launched by an excess of RNS, could cause DNA damage (Potjewyd et al., 2017) and DNA repair inhibition (Zhou et al., 2016), induce protein nitration, damage membrane proteins and fatty acid, leading to changes of cellular signaling transduction, inflammatory response, and even cell death (Kiss and Szabo, 2005; Pacher et al., 2007; Valko et al., 2007). As known, the central nervous system (CNS) is highly sensitive to oxidative or nitrosative stress due to its high energy requirements, high oxygen consumption, and relative deficiency of antioxidants. Hence, this study aimed to investigate the roles of oxidative and nitrosative stress in PBDE's neurotoxicity, and to provide new evidences for the underlying mechanism and targeted intervention. To this end, we used rat cerebral cortex and primary cultured neurons from rat as *in vivo* and *ex vitro* models to explore the oxidative stress, nitrosative stress, and antioxidation changes following BDE-153 treatment, which is based on the knowledge that BDE-153 possesses the highest affinity to brain, and is the hardest to be metabolized in human and mice among the predominant PBDE congeners (BDE-47, BDE-99, BDE-100, and BDE-153) in human (Lupton et al., 2009; Staskal et al., 2006).

2. Materials and methods

2.1. Chemicals and reagents

2, 2', 4, 4', 5, 5'-hexabrominated diphenyl ether (BDE-153, purity 99.9% by GC/MS) was purchased from AccuStandard, Inc. (New-Haven, CT, USA). Rabbit polyclonal antibody against nNOS (H-299) (sc-8309) was purchased from Santa Cruz Biotechnology, Inc, USA, rabbit monoclonal antibody against Prx I (8499s) and Prx II (ab109367) were from Cell Signaling Technology (Beverly, MA,

USA), and Abcam (Cambridge, MA, USA) respectively. Rabbit β -actin antibody was purchased from BOSTER Biological Engineering Co. (Wuhan, Hubei, China). One Step SYBR PrimeScript RT-PCR Kit was purchased from Takara Biotechnology Co. (Dalian, Liaoning, China). N-Acetyl-L-cysteine (NAC, $\geq 99\%$ TLC) and N-Nitro-L-arginine (L-NNA, $\geq 98\%$ TLC) were purchased from Sigma Aldrich, Co (China).

2.2. Animals and treatment

Ten nulliparous pregnant Sprague-Dawley rats (aged 10 weeks) from the Animal Experiment Center of Shanxi Medical University (license number: 754) were individually housed in a standard environment (20–22 °C temperature, 40–70% humidity, and 12/12 h cycle of light and dark) since the pregnant day. Each rat had free access to tap water and standard lab chew pellets (GB 14924.3-2010, obtained from the Animal Experiment Center of Shanxi Medical University). The birthday was documented as postnatal day 0 (PND 0). All the procedures were conducted in accordance with the National Institutes of Health Guide for Care and Use of Laboratory Animals. As we previously described (Zhang et al., 2017b), a total of 60 male pups from 10 litters, average 6 pups/litter, were randomly assigned into four groups ($n = 15$ /group) according to their body weights as follow: olive oil control group, three treated groups at doses of 1, 5, and 10 mg/kg BDE-153, respectively. Pups were administrated once with olive oil or BDE-153 solution at 0.1 mL/10 g body weight via intraperitoneal injection (ip) at PND 10. Pup siblings stayed with their mother until weaning, followed by being co-caged (6/cage) with their partners in the same treated group. Rat pups were routinely fed, weighed, and recorded their food and water consumption daily until euthanasia at PND 70. The animal experimental protocol was approved by the Ethics Review Committee for Animal Research of Shanxi Medical University. BDE-153 was prepared in olive oil solution as previously described (Zhang et al., 2017b), and the dose range was set based on our preliminary experiments and the referenced LOAEL (the lowest observed adverse effect level) 0.9 mg/kg in neonatal mice (Viberg et al., 2003).

2.3. Sampling

At PND 70, rats were anesthetized with sodium pentobarbital and euthanized by decapitation. The brains were carefully removed, instantly weighed and isolated the cerebral cortex on a cold ice. Single cell suspensions were individually obtained from cortical tissues of 6 rats in each group, and were immediately determined the apoptosis and ROS levels using flow cytometry. Brain tissues from 3 individual pups out of each group were fixed overnight by immersing in neutral buffered formaldehyde solution, embedded in paraffin, and sectioned (5 μ m thick) for nNOS immunohistochemistry following the standard procedures. Individual cortical tissues from the remaining 6 pups in each group were collected and stored at -80 °C for determination of mRNA and protein levels, or kinase activity according to the manufacturer's protocol.

2.4. Primary neuron culture, identification and treatment

Primary neurons were cultured as previously described with some modifications (Kaech and Banker, 2006; Brewer and Torricelli, 2007). Briefly, cerebral cortical tissues were dissected under sterile conditions from neonatal SD rat pups (PND 0–3), and the meninges and blood vessels were removed. Single cell suspensions were obtained via digestion using 0.25% trypsin for 10 min at 37 °C and filtration through a 200- μ m mesh cell. Single cell suspensions were suspended in Dulbecco's Modified Eagle

Medium (DMEM) medium containing 10% fetal bovine serum, 10% horse serum and 100 U/mL penicillin-streptomycin, seeded in a culture plate or flask pre-coated with poly-L-lysine (0.1 mg/mL) at 5×10^5 cells/mL density, and subsequently incubated in a humidified incubator with 5% CO₂ at 37 °C. Cytosine arabinoside (a final concentration of 2.5 μM) was added into the medium after 48 h incubation and maintained for 12 h to prevent glial cell proliferation. Neurons were cultured for 7 days. On the 5th day, primary neurons were identified using the specific cytoskeletal protein β-tubulin III. Comparable well-grown and 80–90% confluent neurons out of the same batch were classified and treated for 48 h with blank (medium), dimethyl sulfoxide (DMSO, solvent control), or BDE-153 at three dosage levels of 10, 20, and 40 μM, respectively. DMSO (Sigma-Aldrich) was accounted for 0.3% (v/v) of the total incubation medium, which was regarded as safe to cell (Makita and Sandborn, 1971). After treatment for 48 h, the supernatants were collected for detecting the LDH leakage, and the primary neurons were harvested for the determination of mRNA and protein levels, or kinase activities.

To obtain a solid evidence of the intervention effects targeted oxidative or nitrosative stress in the neurotoxicity following BDE-153 treatment, we pretreated primary neurons with ROS scavenger N-Acetyl-L-cysteine (NAC, ≥99% TLC, Sigma-Aldrich) or NO scavenger N-Nitro-L-arginine (L-NNA, ≥98% TLC, Sigma-Aldrich) at 30 min prior to the 20 μM BDE-153 treatment, and then determined the variations of neurotoxic effects, oxidative stress, nitrosative stress, and antioxidation in primary neurons induced by BDE-153 treatment.

BDE-153 was freshly prepared as a stock solution in DMSO and diluted with serum-free DMEM medium to make different concentrations (0, 10, 20, and 40 μM) prior to each experiment. NAC and L-NNA were freshly dissolved in serum-free DMEM medium. The treating doses were selected based on our preliminary experiment.

2.5. Apoptosis and ROS determination

Single cell suspension was obtained from individual prefrontal cortex tissue or primary neurons via digestion and filtration, and was categorized into two copies. One copy was labeled with fluorescein isothiocyanate (FITC)-conjugated Annexin V and propidium iodide (PI) (Nanjing KeyGEN Biotech, China) at a density of 1×10^5 cells/mL for 15 min in the dark. Apoptotic cells were detected using FACScan flow cytometry (Becton Dickinson, USA) at 488 nm wavelength, and were analyzed using Cell Quest Software (Becton Dickinson, USA).

Another copy of single cell suspensions from cortices or primary neurons were immediately incubated with a final concentration of 1 μM 2',7'-dichlorofluorescein diacetate (DCFDA, Beyotime, China) in the dark for 30 min at a density of 1×10^5 cells/mL. The positive or negative control was added ROSUP (Beyotime, China) or phosphate buffer instead of cells according to the manufacturer's instruction. After centrifugation twice in phosphate buffer, the cell suspension was determined ROS levels using FACScan flow cytometry (Becton Dickinson, USA) at 488 nm wavelength, and were analyzed the mean fluorescence intensity (MFI) using Cell Quest Software (Becton Dickinson, USA).

2.6. LDH activity, neurotrophin contents, and cholinergic enzyme activity

Rat cortices or primary neurons were homogenized using a glass homogenizer, and the homogenate supernatants were obtained through centrifugation. The supernatants were determined the lactate dehydrogenase (LDH) activity using spectrophotometric

method according to the manufacturer's instruction, the contents of brain-derived neurotrophic factor (BDNF), glial cell line-derived neurotrophic factor (GDNF), nerve growth factor (NGF), neurotrophin-3 (NT-3) and neurotrophin-4 (NT-4), and the enzyme activities of choline acetyltransferase (ChAT) and acetylcholinesterase (AChE) using enzyme-linked immunosorbent assay (ELISA) according to the instructions of kits (Shanghai Jianglai Biological Technology, China).

2.7. MDA, NO and nNOS contents

The homogenate supernatants from rat cortices or primary neurons were determine the malondialdehyde (MDA) contents following the manufacturer's instructions (Nanjing Jiancheng Bioengineering Institute, China), the NO content and nNOS activity according to the instructions of kits (Shanghai Jianglai Biological Technology, China).

2.8. nNOS mRNA using quantitative PCR (QPCR) analysis

Total RNA was extracted from cortical tissues or primary neurons using RNAiso Plus (Takara Biotechnology Co., LTD, China), and eligible for the subsequent experiment when the purity (A260/280 ratio) reached to 1.8–2.0. Total RNA (5 μg) was reversely transcribed into cDNA using the One Step SYBR PrimeScript RT-PCR Kit (Takara Biotechnology Co., LTD, China), and cDNA (50 ng) was amplified in a 25 μL reaction system consisting of 12.5 μL 2 × PCR MasterMix, 0.4 μM forward and reverse primers, and RNase free water. The PCR amplification was performed using the BIOER LineGene 9600 PCR System (BIOER, China) as follows: one cycle at 94 °C for 10 s, followed by 40 two-step cycles at 94 °C for 5 s, and 60 °C for 40 s for amplification curve, and then from 65 °C to 90 °C for dissociation curve. The housekeeping gene β-actin was used as an endogenous control to normalize the target mRNA quantification. Each sample was performed in duplicate and the initial mRNA amount was calculated using the $2^{-\Delta\Delta C_t}$ method. Table 1 showed the primer's sequences used in the QPCR amplification.

2.9. nNOS protein using western-blotting

Homogenates were obtained from cortical tissue or neurons in RIPA lysis buffer containing a protease inhibitor phenylmethylsulfonyl fluoride (PMSF, 1 mM) using an ultrasonic disruptor, and then the supernatants were obtained through centrifugation (14,000 rpm) at 4 °C for 15 min. Total protein concentration was quantified using the enhanced bicinchoninic acid (BCA) protein assay kit (Beyotime Institute of Biotechnology, China). Protein samples (~30 μg) in the supernatant were run on a 10% polyacrylamide gel, transferred to a nitrocellulose membrane, and blocked with 5% non-fat milk for 2 h at room temperature. The membrane was followed by incubation with primary antibody

Table 1
Primer sequences of rats' mRNA and product size (bp).

Primer	Sequence (5'-3')	Size(bp)
nNOS-F	5'-CCTATGCCAAGACCCTGTGTGA-3'	132
nNOS-R	5'-CATTGCCAAAGGTGCTGGTG-3'	
Prx I-F	5'-CCGCTCTGTGGATGAGATTCTG-3'	195
Prx I-R	5'-CTTCTGGCTGCTCAAAGCTGTC-3'	
Prx II-F	5'-TTTAGCGACCACGCTGAGGAC-3'	181
Prx II-R	5'-ACACGCCGTAATCTGGGACA-3'	
β-actin-F	5'-GGAGATTACTGCCCTGGCTCTA-3'	150
β-actin-R	5'-GACTCATCGTACTCCTGCTGCTG-3'	

F: forward primer; R: reverse primer.

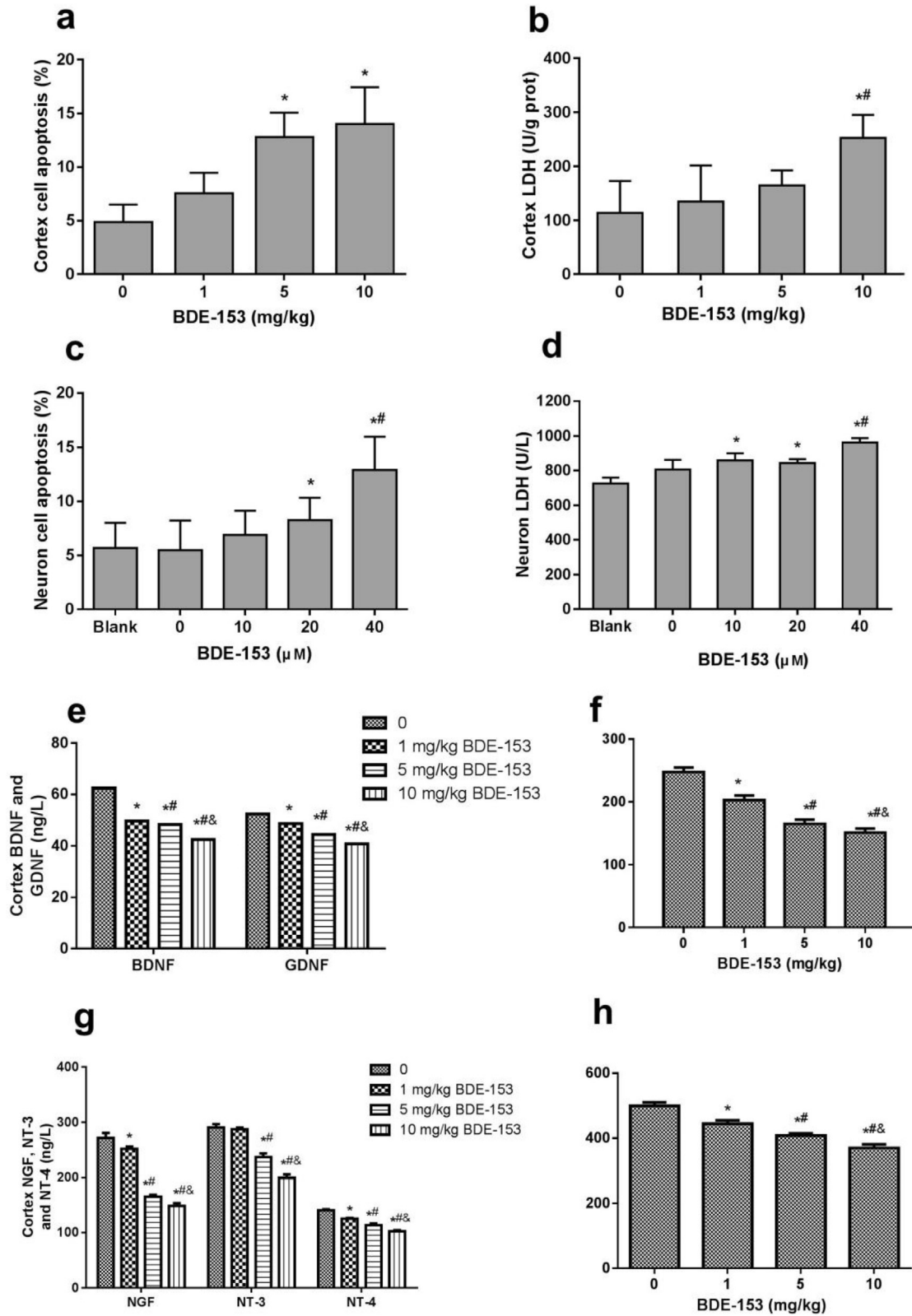


Fig. 1. Neurotoxic effects in cerebral cortex and primary neurons in rats following BDE-153 treatment. Panel a: Cell apoptosis rates (Annexin V⁺/PI⁺) in cerebral cortex, Panel b: LDH activity (U/mg prot) in cerebral cortex, Panel c: Cell apoptosis rates (Annexin V⁺/PI⁺) in primary neurons, Panel d: LDH leakage (U/L) in primary neurons. Panel e: Contents of BDNF and GDNF (ng/L) in cerebral cortex, Panel f: ChaT Activity (ng/L) in cerebral cortex, Panel g: Contents of NGF, NT-3 and NT-4 (ng/L) in cerebral cortex, and Panel h: AChE activity (U/mg prot) in cerebral cortex. The 0 group indicates the untreated group or solvent control, which is only treated by the solvent of olive in the cerebral cortex, or DMSO in primary neurons, but not treated by any dose of BDE-153. *: $P < 0.05$ vs. the untreated group; #: $P < 0.05$ vs. the BDE-153-treated group at 1 mg/kg in cortex or the BDE-153-treated group at 10 μ M in primary neurons.

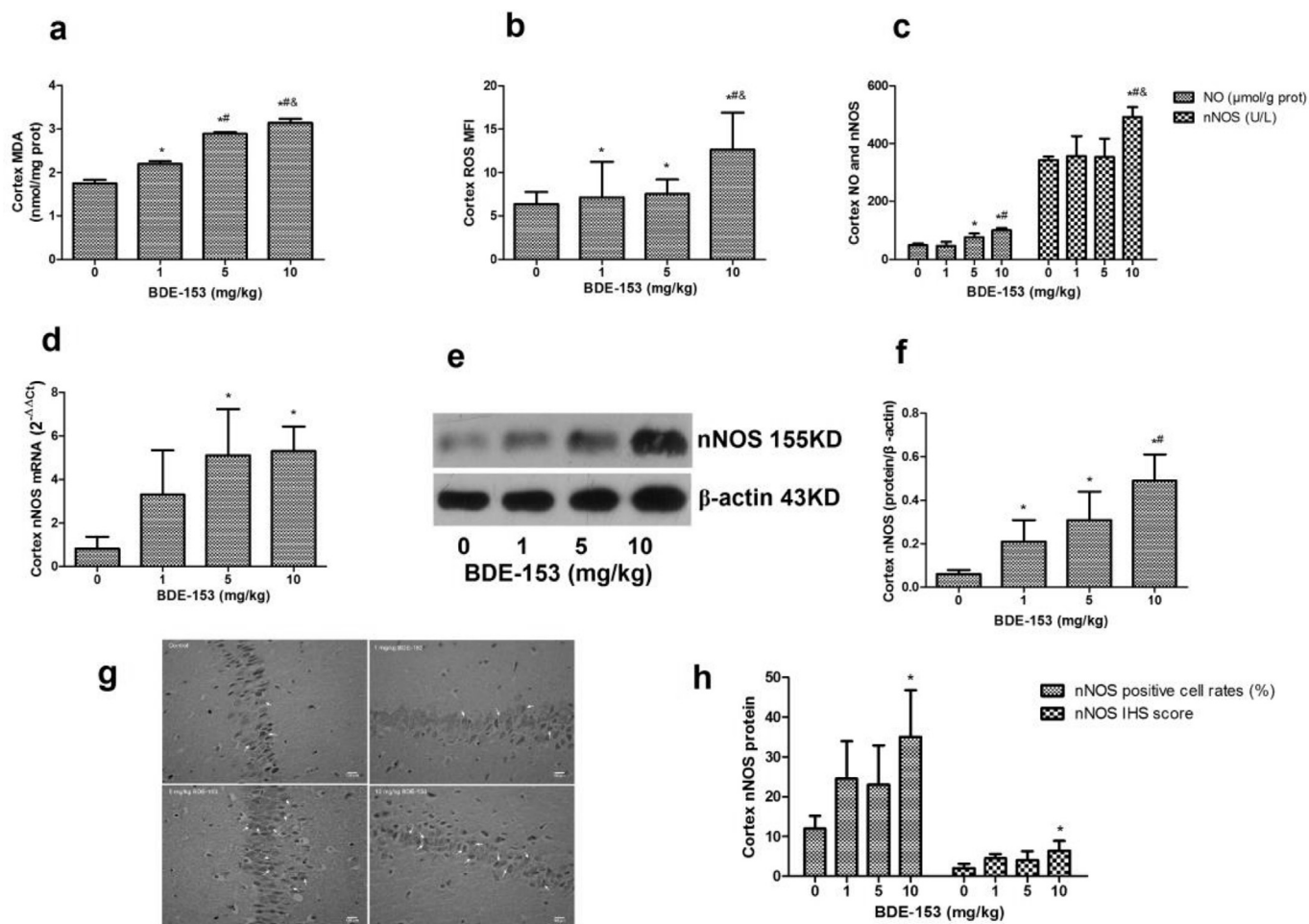


Fig. 2. Oxidative and nitrosative stress in the cerebral cortex in rats following BDE-153 treatment. Panel a: Cerebral cortex MDA content (nmol/mg prot), Panel b: Cerebral cortex ROS mean fluorescence intensity (MFI), Panel c: NO content ($\mu\text{mol/g prot}$) and nNOS activity (U/L) in cerebral cortex, Panel d: Cerebral cortex nNOS mRNA levels, Panel e: Western-blotting bands of nNOS in rats' cerebral cortex following treatment with 0, 1, 5, and 10 mg/kg BDE-153, Panel f: nNOS protein levels in rats' cerebral cortex, Panel g: representative immunohistochemistry images of nNOS in cerebral cortex (arrows indicate the nNOS-positive cells), and Panel h: Cerebral cortex nNOS positive cell rate (%) and nNOS immunohistochemical score (IHS). The untreated group or solvent control was indicated as 0 in the horizontal axis, which is not treated by any dose of BDE-153, but only treated by the olive solvent in rats. *: $P < 0.05$ vs. the untreated group; #: $P < 0.05$ vs. the BDE-153-treated group at 1 mg/kg in cerebral cortex in rats; &: $P < 0.05$ vs. the BDE-153-treated group at 5 mg/kg in cerebral cortex in rats.

nNOS1(H-299)(sc-55521, 1:500) overnight at 4°C , followed by a wash step and a subsequent incubation with secondary antibodies (biotinylated and streptavidin horseradish peroxidase-conjugated secondary anti-mouse antibody, 1:3000) for 2 h at room temperature. The blots were visualized on X-ray film using a super enhanced chemical luminescence kit (Applygen Technologies Inc, China) and documented into images. Each assay was repeated 3 times and yielded in an average value. Protein expression level was expressed as the target protein ratio to reference protein β -actin.

2.10. nNOS immunohistochemistry or immunofluorescence assay

To examine protein expressions in rat's brain, tissue sections ($5\ \mu\text{m}$ thick) orderly underwent routine deparaffinization, rehydration, peroxidase inactivation, antigen retrieval, and permeabilization. All procedures were performed in a humid chamber. The sections were blocked with 3% goat serum, incubated with primary antibody (nNOS, 1:70) overnight at 4°C , followed by a wash step and a subsequent incubation with secondary antibody (1:100) for 1 h at room temperature. The target protein was visualized with 3, 3'-diaminobenzidine (DAB) and counterstained with

hematoxylin. Following dehydration, sections were sealed with a cover slip using neutral resins. Negative control sections contained phosphate buffer instead of the primary antibody. Each slide was photographed the immunohistochemistry (IHS) images under an optical microscope, and an IHS score was obtained for analysis using Image-Pro Plus (Media Cybernetics Co. USA).

Primary neurons were grown in cover slips pre-coated with poly-L-lysine, fixed using 4% paraformaldehyde for 30 min at 4°C , followed by a rinse step and permeabilization with 0.1% Triton X-100, and then blocked with 3% bovine serum albumin (BSA) for 30 min. The slides were incubated with primary antibody (nNOS, 1:50) overnight at 4°C in a humid chamber, and followed by a rinse and a subsequent incubation with FITC-conjugated secondary antibody (1:100) for 2 h at 37°C , and then counterstained with 4, 6-diamidino-2-phenylindole (DAPI) and sealed. Negative control slide contained phosphate buffer instead of the primary antibody for quality control purpose. Images were examined and photographed under an OLYMPUS BX51 fluorescence microscope (OLYMPUS, Japan). The mean fluorescence intensity (MFI) for each slide was measured using Image J (National Institutes of Health, USA).

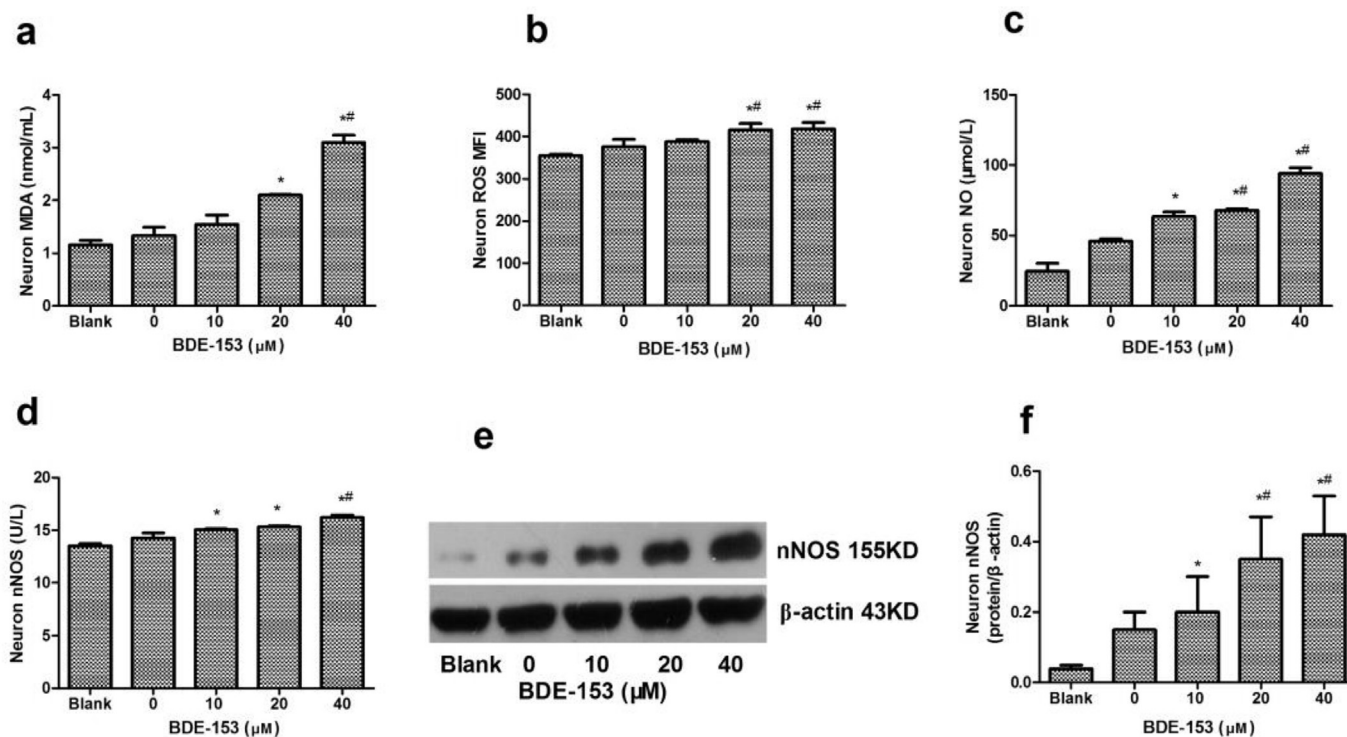


Fig. 3. Oxidative and nitrosative stress in primary neurons following BDE-153 treatment. Panel a: Primary neuron MDA content (nmol/mL), Panel b: Primary neuron ROS mean fluorescence intensity (MFI), Panel c: Primary neuron NO content ($\mu\text{mol/L}$), Panel d: Primary neuron nNOS activity (U/L), Panel e: Western-blotting bands of nNOS in rats' primary neurons following treatment with blank, solvent (DMSO), and BDE-153 at doses of 10, 20 and 40 μM ; Panel f: Primary neurons nNOS protein levels. The untreated group or solvent control was indicated as 0 in the horizontal axis, which is only treated by the solvent of DMSO in primary neurons, but not treated by any dose of BDE-153. *: $P < 0.05$ vs. the untreated group; #: $P < 0.05$ vs. the 10 μM BDE-153 treated group in cultured primary neuron.

2.11. SOD, GSH, Prx I and Prx II levels

As mentioned above, the homogenate supernatants obtained from prefrontal cortices and primary neurons were prepared for measuring the contents of superoxide dismutase (SOD) and glutathione (GSH) according to the manufacturer's protocols, and the mRNA levels in peroxiredoxin I (Prx I) and peroxiredoxin II (Prx II) using QPCR, and the protein levels in Prx I and Prx II using western-blotting, immunofluorescence assay and ELISA methods mentioned above. The primer sequences for Prx I and Prx II mRNA amplification were given in Table 1, and the primary antibodies of Prx I (Cell Signaling Technology, 8499s) and Prx II (Abcam, Ab109367) were both 1:1000 in western-blotting, and were 1:70 in immunofluorescence assay.

2.12. Statistical analysis

Data were presented as mean \pm standard deviation (SD). One-way analysis of variance (ANOVA) was employed for multiple comparison, and followed by the least significant difference (LSD) test for comparison between any two means using Statistical Program for Social Sciences (SPSS) Statistics 17.0 software (International Business Machines Corporation, Almonk, USA). A two-sided p value of 0.05 was considered statistically significant for all tests.

3. Results

3.1. Neurotoxic effects

Compared to the untreated groups (solvent controls), BDE-153 treatment decreased the body weights and the brain/body weight ratios at the end of 2 months of treatment, but the difference was

not significant (See supplement materials, Fig. S1). BDE-153 treatment significantly increased cell apoptotic rate (at 5 and 10 mg/kg) (Fig. 1a) and LDH activity (at 10 mg/kg) (Fig. 1b) in prefrontal cerebral cortex in rats, and LDH activity was significantly higher in the 10 mg/kg BDE-153 group than in the 1 mg/kg BDE-153 group. Similarly, BDE-153 treatment significantly increased cell apoptosis (at 20 and 40 μM) (Fig. 1c) and LDH leakage (at 10, 20, and 40 μM) (Fig. 1d) in primary neurons. When compared to the 10 μM BDE-153 treated group, cell apoptosis and LDH activity were significantly increased following the 40 μM BDE-153 treatment.

Moreover, when in comparison with the untreated group, BDE-153 treatment significantly decreased the contents of BDNF, GDNF, NGF, and NT-4 (at 1, 5, and 10 mg/kg) (Fig. 1e and g), and the NT-3 content (at 5 and 10 mg/kg) (Fig. 1g) in the cortex of rats, and significantly inhibited ChaT and AChE enzyme activities (at 1, 5, and 10 mg/kg) (Fig. 1f and h) as well. Additionally, the neurotrophin contents and cholinergic enzyme activities were significantly depressed in primary neurons following BDE-153 treatment (See supplement materials, Fig. S2).

3.2. Oxidative and nitrosative stress

Compared to the untreated group, BDE-153 treatment significantly increased the MDA and ROS levels (at 1, 5, and 10 mg/kg) in rats' cortex (Fig. 2a and b), NO contents (at 5 and 10 mg/kg), and nNOS activity (at 10 mg/kg dose) (Fig. 2c). When in comparison with the 1 mg/kg BDE-153 treated group, BDE-153 treatment significantly increased the levels of MDA (at 5 and 10 mg/kg), ROS, NO, and nNOS (at 10 mg/kg) in the cerebral cortex of rats. And MDA, ROS and nNOS were significantly higher in the 10 mg/kg BDE-153 treated group than those in the 5 mg/kg BDE-153 treated group. Furthermore, cortex nNOS at mRNA and protein levels were

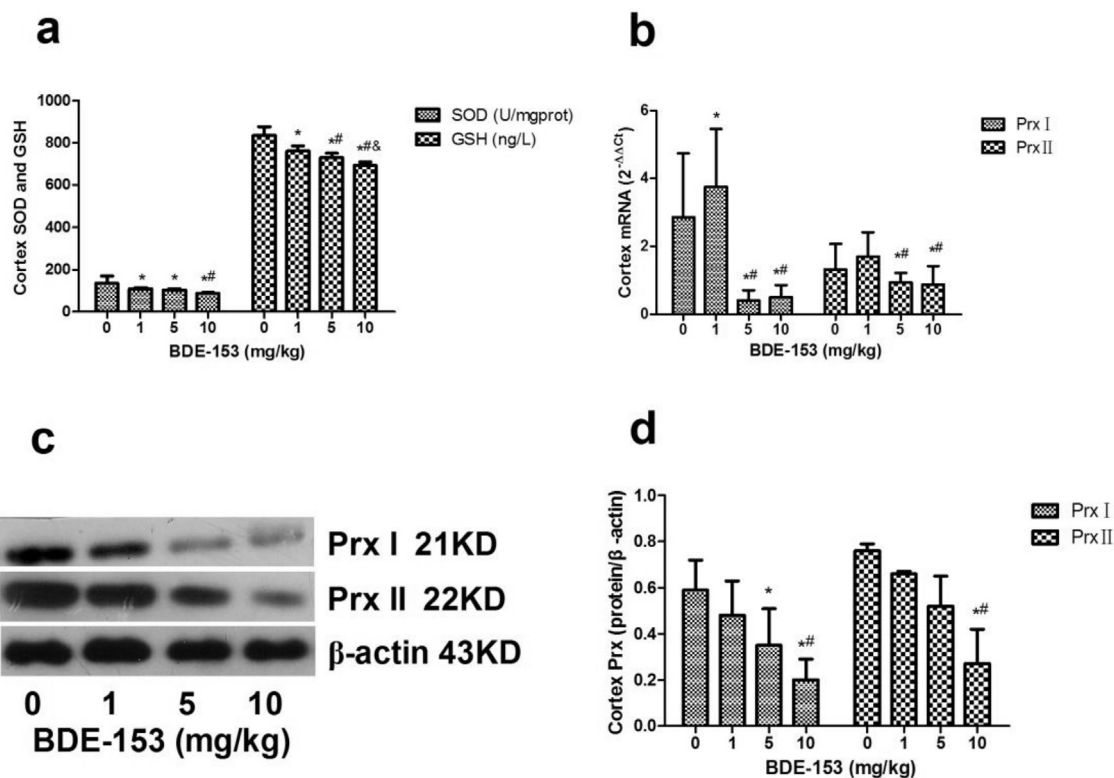


Fig. 4. Antioxidation in cerebral cortex in rats following BDE-153 treatment. Panel a: Cerebral cortex SOD activity (U/mg prot) and GSH content (ng/L), Panel b: Cerebral cortex mRNA levels of Prx I and Prx II, Panel c: Western-blotting bands of Prx I and Prx II in rats' cerebral cortex following treatment with 0, 1, 5, and 10 mg/kg BDE-153, Panel d: Prx I and Prx II protein levels in rats' cerebral cortex. The untreated group or solvent control was indicated as 0 in the horizontal axis, which is only treated by the solvent of olive in the cerebral cortex of rats, but not treated by any dose of BDE-153. *: $P < 0.05$ vs. the untreated group; #: $P < 0.05$ vs. the 1 mg/kg BDE-153 treated group in cerebral cortex in rats.

significantly increased following BDE-153 treatment, as manifested by the increased mRNA (at 5 and 10 mg/kg) (Fig. 2d), protein expression (at 1, 5, and 10 mg/kg) in western blotting (Fig. 2e and f), and nNOS positive cell rates and IHS score (at 10 mg/kg) in immunohistochemistry assay (Fig. 2g and h).

In cultured primary neurons following BDE-153 treatment, the levels of MDA and ROS were significantly increased (at 20 and 40 μ M) (Fig. 3a and b), and the NO content, nNOS activity and protein were significantly increased (at 10, 20, and 40 μ M) (Fig. 3c–f) as compared to the untreated group. When in comparison with the 10 μ M BDE-153 treated group, levels of ROS, NO content and nNOS protein were significantly increased in the 20 and 40 μ M BDE-153 group, and MDA content and nNOS activity were significantly higher in the 40 μ M BDE-153 treated group.

3.3. Antioxidation and denitrication

Compared to the untreated group, BDE-153 treatment significantly decreased the levels of SOD and GSH in the cerebral cortex of rats at doses of 1, 5, and 10 mg/kg (Fig. 4a), reduced Prx I and Prx II at mRNA levels (at 5 and 10 mg/kg) (Fig. 4b), and protein levels in Prx I (at 5 and 10 mg/kg) and Prx II (at 10 mg/kg) (Fig. 4c and d). When in comparison with the 1 mg/kg BDE-153 treated group, the levels of GSH, Prx I and Prx mRNA levels in cerebral cortex were significantly decreased in the 5 and 10 mg/kg BDE-153 treated groups, and SOD activity, Prx I and Prx II protein levels were significantly declined in the 10 mg/kg BDE-153 treated group.

Similar changes appeared in primary neurons following BDE-153 treatment. As compared to the untreated neurons, the contents of SOD and GSH in primary neurons were significantly

decreased following BDE-153 treatment at all three doses, and were significantly lower in the 20 and 40 μ M BDE-153 groups than in the 10 μ M BDE-153 group, significantly lower in the 40 μ M BDE-153 group than in the 20 μ M BDE-153 group (Fig. 5a and b). Compared to the untreated group, BDE-153 treatment had significantly decreased neuron's Prx I mRNA at doses of 20 and 40 μ M, and Prx II mRNA at all three doses (10, 20 and 40 μ M) (Fig. 5c). As compared to the 10 μ M BDE-153 group, Prx I mRNA was statistically reduced in primary neurons treated by 20 and 40 μ M doses of BDE-153, and Prx II mRNA was significantly decreased in primary neurons treated by BDE-153 at 40 μ M. As compared to the untreated group, Prx I and Prx II protein contents and expression were significantly decreased in cultured primary neurons following BDE-153 treatment, as demonstrated by the decreased protein contents in Prx I (at 20 and 40 μ M) and Prx II (at 10, 20 and 40 μ M) (Fig. 5d), and the depressed protein expressions in Prx I and Prx II at all three doses (Fig. 5e and f); When in comparison with the 10 μ M BDE-153 group, Prx I and Prx II protein expressions were significantly reduced in primary neurons treated by 40 μ M BDE-153. Additionally, compare to the untreated primary neurons, the mean immunofluorescence index (MFI) was significantly decreased in primary neurons following BDE-153 treatment in Prx I (at 20 and 40 μ M) and Prx II (at 10, 20 and 40 μ M) (Fig. 5g, and see supplement materials, Figs. S3–4).

3.4. Intervention effects of NAC or N-LLA targeted oxidative or nitrosative stress

When neurons were pretreated with NAC (500 μ M, ROS scavenger) or N-LLA (100 μ M, NO scavenger) at 30 min prior to the BDE-

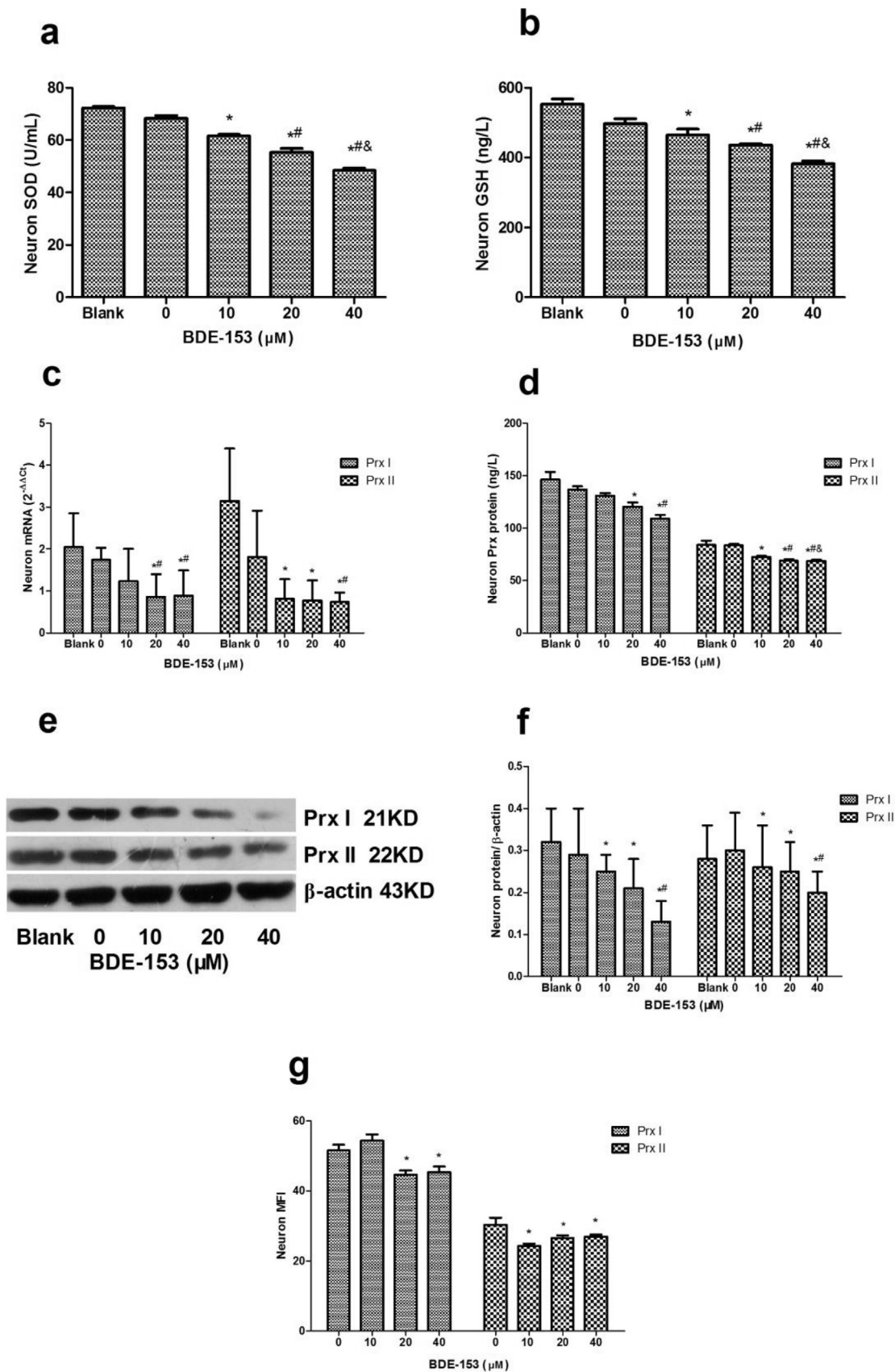


Fig. 5. Antioxidation in primary neurons following BDE-153 treatment. Panel a: Primary neuron SOD activity (U/mL), Panel b: Primary neuron GSH content (ng/L), Panel c: Primary neuron Prx I and Prx II mRNA levels, Panel d: Primary neuron Prx I and Prx II contents (ng/L), Panel e: Western-blotting bands of Prx I and Prx II in rats' primary neurons following treatment with blank, 0, 10, 20, and 40 μM BDE-153, Panel f: Primary neurons Prx I and Prx II protein levels. Panel g: Primary neurons Prx I and Prx II protein mean fluorescence intensity (MFI). The untreated group or solvent control was indicated as 0 in the horizontal axis, which is only treated by the solvent of DMSO in primary neurons, but not treated by any dose of BDE-153. *: $P < 0.05$ vs. the untreated group; #: $P < 0.05$ vs. the 10 μM BDE-153 treated group in primary neuron in rats.

153 treatment, cell survival was reverted in the pretreated groups following BDE-153 treatment when compared to the only BDE-153 treatment, as manifested by the significant decrements in LDH and apoptosis rate (Fig. 6a and b), and the significant increases in contents of BDNF, GDNF, NGF, NT-3, and NT-4 protein (Fig. 6c–g), and in activities of ChaT and AChE (Fig. 6h and i). Compared to the only BDE-153 treated group, the levels of MDA, NO, SOD, Prx I protein were significantly recovered following the N-LLA or NAC pretreatment (Fig. 7a–d), and Prx II protein levels were significantly reverted (Fig. 7e). A more decline in Prx II protein levels following the NAC pretreatment may implicate a similar action site shared by Prx II and NAC.

4. Discussion

The present study comprehensively investigated the role of oxidative/nitrosative stress in neurotoxicity following BDE-153 treatment, demonstrated that oxidative/nitrosative stress occurred and the antioxidation system was impaired in the cerebral cortex and primary neurons in rats, and the neurotoxicity could be attenuated by the ROS or NO scavenger in primary neurons.

The neurotoxicity of BDE-153 had been demonstrated as cognitive dysfunction, disrupted spontaneous behavior, hippocampus neuron apoptosis, depressed neurotrophin contents, and inhibited cholinergic enzymes in adult rats' cerebral cortex in our previous publications (Zhang et al., 2013, 2017b, 2018). Oxidative/nitrosative stress is the result of a disequilibrium in oxidant/antioxidant which results from continuous increase of ROS and RNS production, an impaired antioxidant system, or both (Sener et al., 2003). In the present study, oxidative/nitrosative stress occurred inside neuronal cells following BDE-153 treatment, as indicated by the increased levels of ROS, MDA, NO, and nNOS mRNA and protein, and the decreased SOD activity and GSH level in the cerebral cortex and primary neurons in rats. On the other hand, the antioxidant defense systems were notably impaired, as manifested by the significant decreased SOD activity, GSH level, and the significant suppressed Prx I and Prx II mRNA and protein levels. Oxidative stress had occurred in primary cultured rat hippocampus neurons treated by BDE-209 (Chen et al., 2010), and in multiple cell lines (L02, Jurkat, Hep G2, and SH-SY5Y) following BDE-47 or BDE-47 metabolites treatment, which appeared as increased ROS level, and decreased SOD activity and GSH level (Zhong et al., 2011; Yan

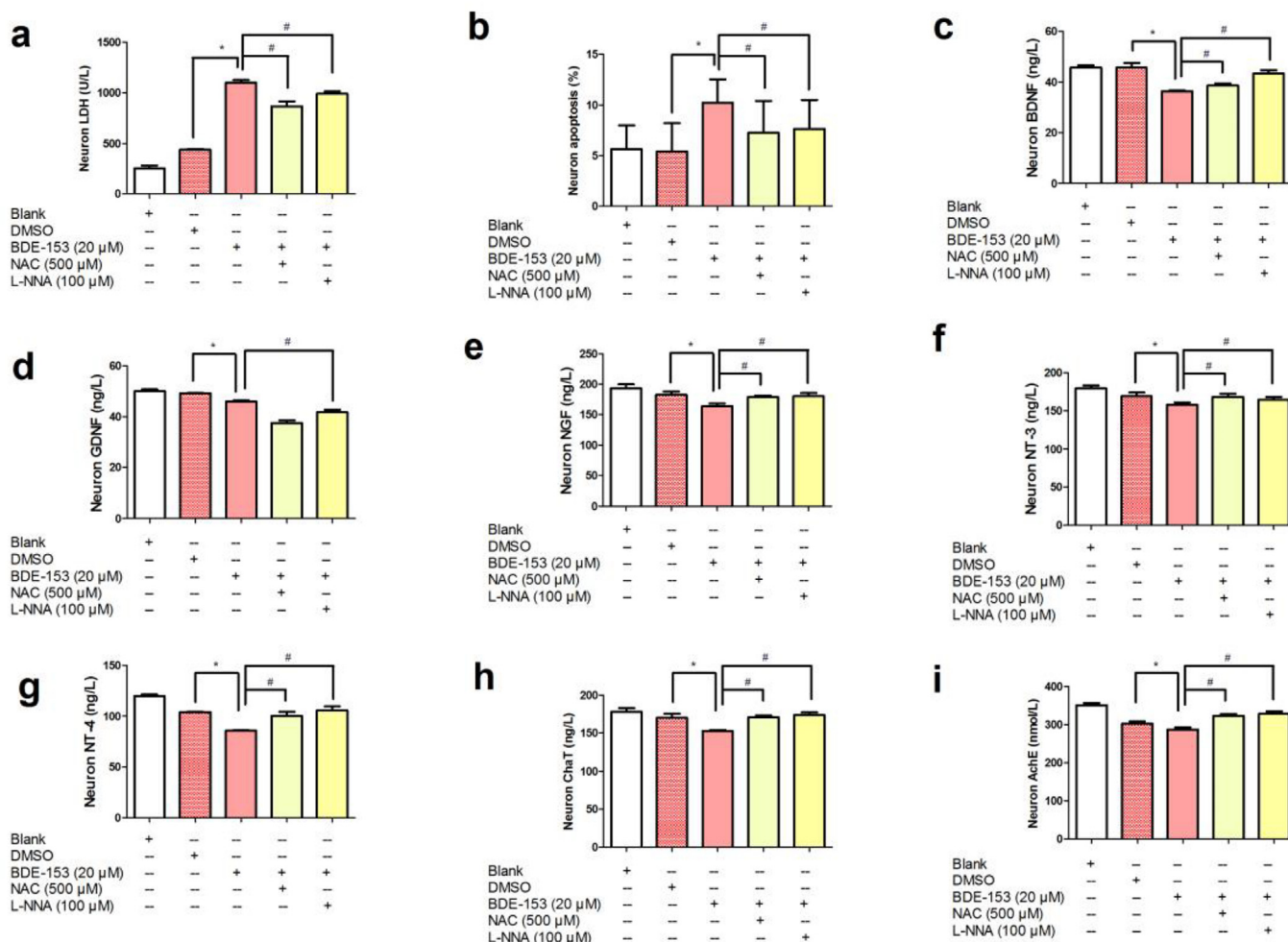


Fig. 6. Intervention effects of NAC or N-LLA on the neurotoxicity of BDE-153 in primary neurons. Panel a: Primary neuron LDH leakage (U/L) when pretreated with inhibitors, Panel b: Primary neuron apoptosis rate (%) when pretreated with inhibitors, Panel c: Primary neuron BDNF content (ng/L) when pretreated with inhibitors, Panel d: Primary neuron GDNF content (ng/L) when pretreated with inhibitors, Panel e: Primary neuron NGF content (ng/L) when pretreated with inhibitors, Panel f: Primary neuron NT-3 content (ng/L) when pretreated with inhibitors, Panel g: Primary neuron NT-4 content (ng/L) when pretreated with inhibitors, Panel h: Primary neuron ChaT activity (ng/L) when pretreated with inhibitors, and Panel i: Primary neuron AChE activity (nmol/L) when pretreated with inhibitors. *: $P < 0.05$ vs. to the DMSO group in primary neurons; #: $P < 0.05$ vs. to the only 20 μM BDE-153 group in primary neurons.

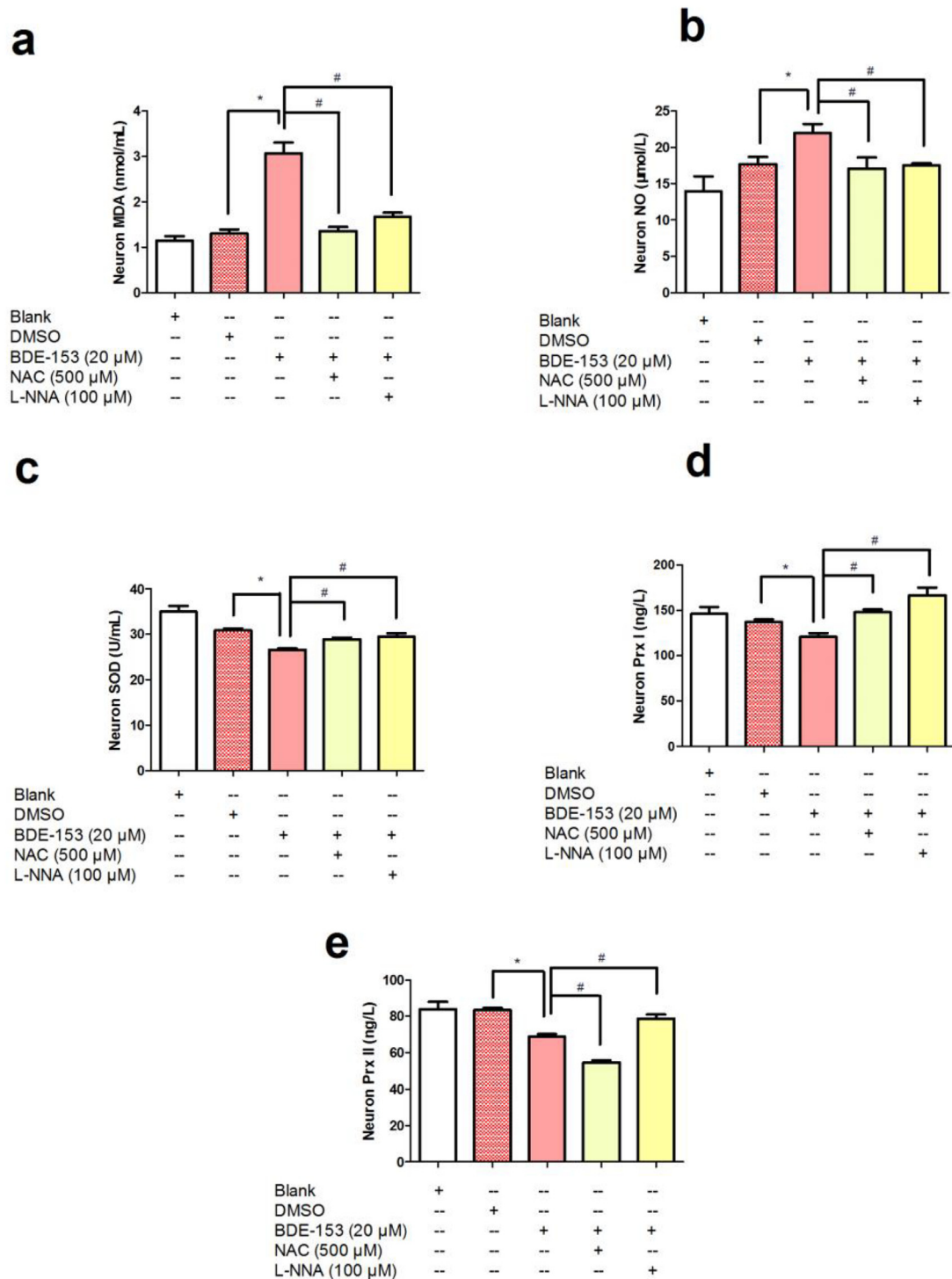


Fig. 7. Intervention effects of NAC or N-LLA on oxidative and nitrosative stress in primary neurons following BDE-153 treatment. Panel a: Primary neuron SOD activity (U/mL) when pretreated with inhibitors, Panel b: Primary neuron NO content (μ mol/L) when pretreated with inhibitors, Panel c: Primary neuron MDA content (nmol/mL) when pretreated with inhibitors, Panel d: Primary neuron Prx I content (ng/L) when pretreated with inhibitors, Panel e: Primary neuron Prx II content (ng/L) when pretreated with inhibitors. *: $P < 0.05$ vs. to the DMSO group in primary neurons; #: $P < 0.05$ vs. to the 20 μ M BDE-153 treated group in primary neurons.

et al., 2011; Liu et al., 2015; Jiang et al., 2012). ROS are capable of initiating and promoting oxidative damage as persistent lipid peroxidation (LPO) (Reiter et al., 2001; Kovacic and Cooksy, 2005), which is known to cause cellular injury via inactivation of membrane enzymes and receptors, depolymerisation of polysaccharide, as well as protein cross-linking and fragmentation (Luqman and

Rizvi, 2006). MDA and SOD have often been clinically treated as matching indicators. SOD is a main free radical scavenger and is considered to be the first line of defense against deleterious effects of ROS since it accelerates the dismutation of superoxide radicals ($O_2^{\cdot-}$) to H_2O_2 , whereas MDA reflects the degree of cell damage caused by free radicals since MDA is an end-product of LPO

(Yelinova et al., 1996).

GSH is a major endogenous antioxidant, and catalyzes the conjugation of reduced glutathione with a variety of exogenous compounds such as toxic carbonyl-, peroxide-, and epoxide-containing metabolites within cells produced by oxidative stress (Beckett and Hayes, 1993; Hayes and Pulford, 1995). In the CNS, the decrease in GSH concentration is associated with the decline in cognition and other brain functions (Currais and Maher, 2013; Mandal et al., 2015), and to increase the GSH concentration in brain, which has become a promising approach for the treatment of brain disorders (Gu et al., 2015). Prx, an unusual antioxidant protein, contains an active site cysteine that is sensitive to oxidation induced by ROS, with crucial roles in protecting cells against oxidative stress and promoting longevity. Prx is used as a biomarker of oxidative stress (Poynton and Hampton, 2014). Mammalian cells express 6 Prx isoforms (Prx I–VI), which are localized to various cellular compartments. Among them, Prx I and Prx II enzymes are mostly present in the cytosolic fraction, play important roles in eliminating H₂O₂, intracellular ROS, and lipid peroxides inside cells (Bae et al., 2007; Kim et al., 2000), and maintain hippocampus synaptic plasticity against oxidative damage (Kim et al., 2011). Prx I gene deficient mice have less reducing activity and are more susceptible to the damage induced by ROS *in vivo* than wild-type mice (Uwayama et al., 2006). The decrements in GSH concentration, Prx I and Prx II mRNA and protein expressions, along with the depressed SOD activities, generally indicate the impaired antioxidation systems following BDE-153 treatment.

Nitrosative stress, closely related to oxidative stress, is caused by overproduction of RNS, the product of superoxide (O²⁻) and NO radical combination, generates peroxynitrite (Halliwell, 1997). NO is a short-lived gas molecule, freely diffuses through aqueous and lipid environments, acts as a neurotransmitter and exists in multiple physiologic and pathologic functions in the mammalian CNS, such as regulating synaptic plasticity via interacting with cyclic GMP (cGMP) (Pigott and Garthwaite, 2016; Haj-Dahmane et al., 2017), neuronal inflammation and neurodegeneration (Shefa et al., 2017; Anaiegoudari et al., 2016). NO is generated from L-arginine under the NOS catalysis, which are composed of 3 isoforms including neuronal NOS (nNOS), inducible NOS (iNOS), and endothelial NOS (eNOS). Then nNOS isoform is predominant in the CNS, and plays a key role in spatial memory formation in rats (Gocmez et al., 2015). The present study indicates that both NO contents and nNOS mRNA and protein expressions were significantly increased in the cerebral cortex and primary neurons in rats following BDE-153 treatment, which are consistent with the increases of NOS activity and NO contents in HepG2 cells following BDE-47 treatment (Hu et al., 2009). NO content is increased in primary cultured neonatal rat hippocampus neurons following BDE-209 treatment (Chen et al., 2010). Aberrant NO levels in the CNS inhibit neurite outgrowth of neurons (Scheiblich and Bicker, 2016), promote mitochondrial dysfunction and cell apoptosis in neuronal cells (Xu et al., 2017), mediate nuclear factor-κB activation and ischemic-related brain damage (Greco et al., 2011), and cause neurodegeneration (Moncada and Bolanos, 2006). High levels of NO production by nNOS activation induce mitochondrial cytochrome c (Cyt-c) release and Bcl-2 down-regulation, lead to apoptosis in PC12 cells (Jiang et al., 2014). And these effects could be effectively inhibited by a highly selective nNOS inhibitor (Jiang et al., 2014).

In this study, preincubation with the N-LLA (NO scavenger) or NAC (ROS scavenger) partially reversed the neurotoxic effects of BDE-153 in primary neurons, as demonstrated by the declined LDH leakage and cell apoptosis, and the increased neurotrophin contents and cholinergic enzyme activities. The finding is consistent with that found in HepG2 or Jurkat cells following BDE-47

treatment (Yan et al., 2011; Hu et al., 2009). Moreover, preincubation with either N-LLA or NAC reduced the MDA and NO contents, simultaneously enhanced the SOD activity and Prx I and Prx II levels. The finding indicates the crosstalk between oxidative and nitrosative stress. It was shown that Prx play crucial roles against nitrosative stress by catalyzing the reduction of peroxynitrite (Abbas et al., 2013). To some extent, oxidative and nitrosative stress were regarded as two branches in the same tree, they interacted with each other via the interlinking molecules, initiated ROS/RNS signaling via the gene network, responsive proteins and post-translational modification (Molassiotis and Fotopoulos, 2011).

In summary, we examined the neurotoxic effects (LDH leakage, cell apoptosis, neurotrophin contents, and cholinergic enzyme activity) in rat's cerebral cortex and primary neurons following BDE-153 treatment, detected the changes of oxidative stress (ROS and MDA contents), nitrosative stress (NO content, nNOS mRNA and protein), and antioxidation (SOD activity, GSH level, and Prx I and Prx II mRNA and protein) *in vivo* and *in vitro*. We also utilized NO or ROS scavenger to pretreat primary neurons *in vitro*, and examined the variations of above neurotoxic effects, oxidation, nitrosation, antioxidation in neurons following BDE-153 treatment. In the end, findings from the present study indicated that both oxidative and nitrosative stress involved in the neurotoxicity of BDE-153, and antioxidation could be the potential targeted intervention.

Funds

This work received the financial support from the National Natural Science Foundation of China (NSFC81973093, 81001258, 31171023), Research Project Supported by Shanxi Scholarship Council of China (2017-059), Personnel Training Project of Shanxi Graduate Joint Training Base (2017JD24), Scientific and Technological Innovation Programs of Higher Education Institutions in Shanxi (STIP201802061).

Conflicts of interest

None.

Appendix A. Supplementary data

Supplementary data to this article can be found online at <https://doi.org/10.1016/j.chemosphere.2019.124602>.

References

- Abbas, K., Riquier, S., Drapier, J.C., 2013. Peroxiredoxins and sulfiredoxin at the crossroads of the NO and H₂O₂ signaling pathways. *Methods Enzymol.* 527, 113–128.
- Anaiegoudari, A., Soukhtanloo, M., Shafei, M.N., Sadeghnia, H.R., Reisi, P., Beheshti, F., Behradnia, S., Mousavi, S.M., Hosseini, M., 2016. Neuronal nitric oxide synthase has a role in the detrimental effects of lipopolysaccharide on spatial memory and synaptic plasticity in rats. *Pharmacol. Rep.* 68 (2), 243–249.
- Bae, J.Y., Ahn, S.J., Han, W., Noh, D.Y., 2007. Peroxiredoxin I and II inhibit H₂O₂-induced cell death in MCF-7 cell lines. *J. Cell. Biochem.* 101 (4), 1038–1045.
- Beckett, G.J., Hayes, J.D., 1993. Glutathione S-transferases: biomedical applications. *Adv. Clin. Chem.* 30, 281–380.
- Brewer, G.J., Torricelli, J.R., 2007. Isolation and culture of adult neurons and neurospheres. *Nat. Protoc.* 2 (6), 1490–1498.
- Chao, H.R., Tsou, T.C., Huang, H.L., Chang-Chien, G.P., 2011. Levels of breast milk PBDEs from southern Taiwan and their potential impact on neurodevelopment. *Pediatr. Res.* 70 (6), 596–600.
- Chen, J., Liufu, C., Sun, W., Sun, X., Chen, D., 2010. Assessment of the neurotoxic mechanisms of decabrominated diphenyl ether (PBDE-209) in primary cultured neonatal rat hippocampal neurons includes alterations in second messenger signaling and oxidative stress. *Toxicol. Lett.* 192 (3), 431–439.
- Chen, A., Yolton, K., Rauch, S.A., Webster, G.M., Hornung, R., Sjodin, A., Dietrich, K.N., Lanphear, B.P., 2014. Prenatal polybrominated diphenyl ether exposures and neurodevelopment in U.S. children through 5 years of age: the HOME study. *Environ. Health Perspect.* 122 (8), 856–862.

- Currais, A., Maher, P., 2013. Functional consequences of age-dependent changes in glutathione status in the brain. *Antioxidants Redox Signal.* 19 (8), 813–822.
- Eskenazi, B., Chevrier, J., Rauch, S.A., Kogut, K., Harley, K.G., Johnson, C., Trujillo, C., Sjodin, A., Bradman, A., 2013. In utero and childhood polybrominated diphenyl ether (PBDE) exposures and neurodevelopment in the CHAMACOS study. *Environ. Health Perspect.* 121 (2), 257–262.
- Gomez, S.S., Yazir, Y., Sahin, D., Karadenizli, S., Utkan, T., 2015. The effect of a selective neuronal nitric oxide synthase inhibitor 3-bromo 7-nitroindazole on spatial learning and memory in rats. *Pharmacol. Biochem. Behav.* 131, 19–25.
- Greco, R., Mangione, A.S., Amantea, D., Bagetta, G., Nappi, G., Tassorelli, C., 2011. I κ B α expression following transient focal cerebral ischemia is modulated by nitric oxide. *Brain Res.* 1372, 145–151.
- Gu, F., Chauhan, V., Chauhan, A., 2015. Glutathione redox imbalance in brain disorders. *Curr. Opin. Clin. Nutr. Metab. Care* 18 (1), 89–95.
- Haj-Dahmane, S., Beique, J.C., Shen, R.Y., 2017. GluA2-Lacking AMPA receptors and nitric oxide signaling gate spike-timing-dependent potentiation of glutamate synapses in the dorsal raphe nucleus. *eNeuro* 4 (3).
- Halliwell, B., 1997. What nitrates tyrosine? Is nitrotyrosine specific as a biomarker of peroxynitrite formation in vivo? *FEBS Lett.* 411 (2–3), 157–160.
- Hammel, S.C., Hoffman, K., Lorenzo, A.M., Chen, A., Phillips, A.L., Butt, C.M., Sosa, J.A., Webster, T.F., Stapleton, H.M., 2017. Associations between flame retardant applications in furniture foam, house dust levels, and residents' serum levels. *Environ. Int.* 107, 181–189.
- Hayes, J.D., Pulford, D.J., 1995. The glutathione S-transferase supergene family: regulation of GST and the contribution of the isoenzymes to cancer chemoprotection and drug resistance. *Crit. Rev. Biochem. Mol. Biol.* 30 (6), 445–600.
- Herbstman, J.B., Sjodin, A., Kurzon, M., Lederman, S.A., Jones, R.S., Rauh, V., Needham, L.L., Tang, D., Niedzwiecki, M., Wang, R.Y., Perera, F., 2010. Prenatal exposure to PBDEs and neurodevelopment. *Environ. Health Perspect.* 118 (5), 712–719.
- Hu, X., Hu, D., Xu, Y., 2009. Effects of tetrabrominated diphenyl ether and hexabromocyclododecanes in single and complex exposure to hepatoma HepG2 cells. *Environ. Toxicol. Pharmacol.* 27 (3), 327–337.
- Jeong, Y., Lee, S., Kim, S., Choi, S.D., Park, J., Kim, H.J., Lee, J.J., Choi, G., Choi, S., Kim, S., Kim, S.Y., Kim, Y.D., Cho, G., Suh, E., Kim, S.K., Eun, S.H., Eom, S., Kim, S., Kim, G.H., Lee, W.C., Choi, K., Kim, S., Moon, H.B., 2014. Infant exposure to polybrominated diphenyl ethers (PBDEs) via consumption of homemade baby food in Korea. *Environ. Res.* 134, 396–401.
- Jiang, C., Zhang, S., Liu, H., Zeng, Q., Xia, T., Chen, Y., Kuang, G., Zhao, G., Wu, X., Zhang, X., Wang, A., 2012. The role of the IRE1 pathway in PBDE-47-induced toxicity in human neuroblastoma SH-SY5Y cells in vitro. *Toxicol. Lett.* 211 (3), 325–333.
- Jiang, J., Duan, Z., Nie, X., Xi, H., Li, A., Guo, A., Wu, Q., Jiang, S., Zhao, J., Chen, G., 2014. Activation of neuronal nitric oxide synthase (nNOS) signaling pathway in 2,3,7,8-tetrachlorodibenzo-p-dioxin (TCDD)-induced neurotoxicity. *Environ. Toxicol. Pharmacol.* 38 (1), 119–130.
- Johnson-Restrepo, B., Kannan, K., 2009. An assessment of sources and pathways of human exposure to polybrominated diphenyl ethers in the United States. *Chemosphere* 76 (4), 542–548.
- Kaech, S., Banker, G., 2006. Culturing hippocampal neurons. *Nat. Protoc.* 1 (5), 2406–2415.
- Kim, H., Lee, T.H., Park, E.S., Suh, J.M., Park, S.J., Chung, H.K., Kwon, O.Y., Kim, Y.K., Ro, H.K., Shong, M., 2000. Role of peroxiredoxins in regulating intracellular hydrogen peroxide and hydrogen peroxide-induced apoptosis in thyroid cells. *J. Biol. Chem.* 275 (24), 18266–18270.
- Kim, S.U., Jin, M.H., Kim, Y.S., Lee, S.H., Cho, Y.S., Cho, K.J., Lee, K.S., Kim, Y.L., Kim, G.W., Kim, J.M., Lee, T.H., Lee, Y.H., Shong, M., Kim, H.C., Chang, K.T., Yu, D.Y., Lee, D.S., 2011. Peroxiredoxin II preserves cognitive function against age-linked hippocampal oxidative damage. *Neurobiol. Aging* 32 (6), 1054–1068.
- Kiss, L., Szabo, C., 2005. The pathogenesis of diabetic complications: the role of DNA injury and poly(ADP-ribose) polymerase activation in peroxynitrite-mediated cytotoxicity. *Mem. Inst. Oswaldo Cruz* 100 (Suppl. 1), 29–37.
- Kovacic, P., Cooksy, A., 2005. Iminine metabolite mechanism for nicotine toxicity and addiction: oxidative stress and electron transfer. *Med. Hypotheses* 64 (1), 104–111.
- Liu, X., Wang, J., Lu, C., Zhu, C., Qian, B., Li, Z., Liu, C., Shao, J., Yan, J., 2015. The role of lysosomes in BDE 47-mediated activation of mitochondrial apoptotic pathway in HepG2 cells. *Chemosphere* 124, 10–21.
- Lupton, S.J., McGarrigle, B.P., Olson, J.R., Wood, T.D., Aga, D.S., 2009. Human liver microsome-mediated metabolism of brominated diphenyl ethers 47, 99, and 153 and identification of their major metabolites. *Chem. Res. Toxicol.* 22 (11), 1802–1809.
- Luqman, S., Rizvi, S.I., 2006. Protection of lipid peroxidation and carbonyl formation in proteins by capsaicin in human erythrocytes subjected to oxidative stress. *Phytother Res.* 20 (4), 303–306.
- Makita, T., Sandborn, E.B., 1971. The effect of dimethyl sulfoxide (DMSO) in the incubation medium for the cytochemical localization of succinate dehydrogenase. *Histochemie* 26 (4), 305–310.
- Mandal, P.K., Saharan, S., Tripathi, M., Murari, G., 2015. Brain glutathione levels—a novel biomarker for mild cognitive impairment and Alzheimer's disease. *Biol. Psychiatry* 78 (10), 702–710.
- Molassiotis, A., Fotopoulos, V., 2011. Oxidative and nitrosative signaling in plants: two branches in the same tree? *Plant Signal. Behav.* 6 (2), 210–214.
- Moncada, S., Bolanos, J.P., 2006. Nitric oxide, cell bioenergetics and neurodegeneration. *J. Neurochem.* 97 (6), 1676–1689.
- Ni, K., Lu, Y., Wang, T., Kannan, K., Gosens, J., Xu, L., Li, Q., Wang, L., Liu, S., 2013. A review of human exposure to polybrominated diphenyl ethers (PBDEs) in China. *Int. J. Hyg. Environ. Health* 216 (6), 607–623.
- Pacher, P., Beckman, J.S., Liaudet, L., 2007. Nitric oxide and peroxynitrite in health and disease. *Physiol. Rev.* 87 (1), 315–424.
- Pigott, B.M., Garthwaite, J., 2016. Nitric oxide is required for L-type Ca²⁺ channel-dependent long-term potentiation in the Hippocampus. *Front. Synaptic Neurosci.* 8, 17.
- Potjewyd, G., Day, P.J., Shangula, S., Margison, G.P., Povey, A.C., 2017. L-beta-N-methylamino-l-alanine (BMAA) nitrosation generates a cytotoxic DNA damaging alkylating agent: an unexplored mechanism for neurodegenerative disease. *Neurotoxicology (Little Rock)* 59, 105–109.
- Poynton, R.A., Hampton, M.B., 2014. Peroxiredoxins as biomarkers of oxidative stress. *Biochim. Biophys. Acta* 1840 (2), 906–912.
- Reiter, R.J., Tan, D.-x., Manchester, L.C., Qi, W., 2001. Biochemical reactivity of melatonin with reactive oxygen and nitrogen species. *Cell Biochem. Biophys.* 34 (2), 237–256.
- Roze, E., Meijer, L., Bakker, A., Van Braeckel, K.N., Sauer, P.J., Bos, A.F., 2009. Prenatal exposure to organohalogenes, including brominated flame retardants, influences motor, cognitive, and behavioral performance at school age. *Environ. Health Perspect.* 117 (12), 1953–1958.
- Scheiblich, H., Bicker, G., 2016. Nitric oxide regulates antagonistically phagocytic and neurite outgrowth inhibiting capacities of microglia. *Dev. Neurobiol.* 76 (5), 566–584.
- Sener, G., Sehirli, A.O., Ayanoglu-Dulger, G., 2003. Melatonin protects against mercury(II)-induced oxidative tissue damage in rats. *Pharmacol. Toxicol.* 93 (6), 290–296.
- Shefa, U., Yeo, S.G., Kim, M.S., Song, I.O., Jung, J., Jeong, N.Y., Huh, Y., 2017. Role of gasotransmitters in oxidative stresses, neuroinflammation, and neuronal repair. *BioMed Res. Int.* 1689341, 2017.
- Shin, M.Y., Lee, S., Choi, H., Jeong, D.I., Moon, H.B., Kim, S., 2017. Placental and lactational transfer of decabromodiphenyl ether and 2,2',4,4'-tetrabromodiphenyl ether in dam-offspring pairs of Sprague-Dawley rats. *Food Chem. Toxicol.* 102, 198–203.
- Staskal, D.F., Hakk, H., Bauer, D., Diliberto, J.J., Birnbaum, L.S., 2006. Toxicokinetics of polybrominated diphenyl ether congeners 47, 99, 100, and 153 in mice. *Toxicol. Sci.* 94 (1), 28–37.
- Tang, J., Zhai, J.X., 2017. Distribution of polybrominated diphenyl ethers in breast milk, cord blood and placenta: a systematic review. *Environ. Sci. Pollut. Res. Int.* 24 (27), 21548–21573.
- Uwayama, J., Hirayama, A., Yanagawa, T., Warabi, E., Sugimoto, R., Itoh, K., Yamamoto, M., Yoshida, H., Koyama, A., Ishii, T., 2006. Tissue Prx I in the protection against Fe-NTA and the reduction of nitroxyl radicals. *Biochem. Biophys. Res. Commun.* 339 (1), 226–231.
- Valko, M., Leibfritz, D., Moncol, J., Cronin, M.T., Mazur, M., Telser, J., 2007. Free radicals and antioxidants in normal physiological functions and human disease. *Int. J. Biochem. Cell Biol.* 39 (1), 44–84.
- Viberg, H., Fredriksson, A., Eriksson, P., 2003. Neonatal exposure to polybrominated diphenyl ether (PBDE 153) disrupts spontaneous behaviour, impairs learning and memory, and decreases hippocampal cholinergic receptors in adult mice. *Toxicol. Appl. Pharmacol.* 192 (2), 95–106.
- Viberg, H., Johansson, N., Fredriksson, A., Eriksson, J., Marsh, G., Eriksson, P., 2006. Neonatal exposure to higher brominated diphenyl ethers, hepta-, octa-, or nonabromodiphenyl ether, impairs spontaneous behavior and learning and memory functions of adult mice. *Toxicol. Sci.* 92 (1), 211–218.
- Xu, Z., Lu, Y., Wang, J., Ding, X., Chen, J., Miao, C., 2017. The protective effect of propofol against TNF-alpha-induced apoptosis was mediated via inhibiting iNOS/NO production and maintaining intracellular Ca²⁺ homeostasis in mouse hippocampal HT22 cells. *Biomed. Pharmacother.* 91, 664–672.
- Xu, B., Wu, M., Wang, M., Pan, C., Qiu, W., Tang, L., Xu, G., 2018. Polybrominated diphenyl ethers (PBDEs) and hydroxylated PBDEs in human serum from Shanghai, China: a study on their presence and correlations. *Environ. Sci. Pollut. Res. Int.* 25 (4), 3518–3526.
- Yan, C., Huang, D., Zhang, Y., 2011. The involvement of ROS overproduction and mitochondrial dysfunction in PBDE-47-induced apoptosis on Jurkat cells. *Exp. Toxicol. Pathol.* 63 (5), 413–417.
- Yelinova, V., Glazachev, Y., Khramtsov, V., Kudryashova, L., Rykova, V., Salganik, R., 1996. Studies of human and rat blood under oxidative stress: changes in plasma thiol level, antioxidant enzyme activity, protein carbonyl content, and fluidity of erythrocyte membrane. *Biochem. Biophys. Res. Commun.* 221 (2), 300–303.
- Zhang, H., Li, X., Nie, J., Niu, Q., 2013. Lactation exposure to BDE-153 damages learning and memory, disrupts spontaneous behavior and induces hippocampus neuron death in adult rats. *Brain Res.* 1517, 44–56.
- Zhang, J., Chen, L., Xiao, L., Ouyang, F., Zhang, Q.Y., Luo, Z.C., 2017. Polybrominated diphenyl ether concentrations in human breast milk specimens worldwide. *Epidemiology* 28 (Suppl. 1), S89–S97.
- Zhang, H., Chang, L., Zhang, H., Nie, J., Zhang, Z., Yang, X., Vuong, A.M., Wang, Z., Chen, A., Niu, Q., 2017. Calpain-2/p35-p25/Cdk5 pathway is involved in the neuronal apoptosis induced by polybrominated diphenyl ether-153. *Toxicol. Lett.* 277, 41–53.
- Zhang, H., Yang, X., Zhang, H., Li, X., Zhang, Z., Hou, L., Wang, Z., Niu, Q., Wang, T., 2018. Neurotrophins and cholinergic enzyme regulated by calpain-2: new insights into neuronal apoptosis induced by polybrominated diphenyl ether-153. *Toxicol. Lett.* 291, 29–38.
- Zhong, Y.F., Wang, L.L., Yin, L.L., An, J., Hou, M.L., Zheng, K.W., Zhang, X.Y., Wu, M.H.,

Yu, Z.Q., Sheng, G.Y., Fu, J.M., 2011. Cytotoxic effects and oxidative stress response of six PBDE metabolites on human L02 cells. *J Environ Sci Health A Tox Hazard Subst Environ Eng* 46 (12), 1320–1327.

Zhou, X., Cooper, K.L., Huestis, J., Xu, H., Burchiel, S.W., Hudson, L.G., Liu, K.J., 2016. S-nitrosation on zinc finger motif of PARP-1 as a mechanism of DNA repair inhibition by arsenite. *Oncotarget* 7 (49), 80482–80492.